

Hidden Order in URu₂Si₂ Unveiled

E. Ressouche,¹ R. Ballou,² F. Bourdarot,¹ D. Aoki,¹ V. Simonet,² M. T. Fernandez-Diaz,³ A. Stunault,³ and J. Flouquet¹

¹*SPSMS, UMR-E CEA/UJF-Grenoble 1, INAC, Grenoble F-38054, France*

²*Institut Néel, CNRS & Université Joseph Fourier, BP166, Grenoble 38042, France*

³*Institut Laue-Langevin, BP 156, 38042 Grenoble Cedex 9, France*

(Received 7 May 2012; published 7 August 2012)

We report on measurements, by polarized neutron elastic scattering, of the magnetization distribution induced in a single crystal of URu₂Si₂ under a magnetic field applied along the tetragonal *c* axis. A subtle change in this distribution, revealed by maximum entropy analysis of the data, is found when the temperature is decreased to the range of the hidden order. An analysis in terms of U⁴⁺ ionic states reveals that this change is a fingerprint of a freezing of rank 5 multipoles, i.e., dotriacontapoles.

DOI: [10.1103/PhysRevLett.109.067202](https://doi.org/10.1103/PhysRevLett.109.067202)

PACS numbers: 75.30.Mb, 61.05.fm, 71.27.+a

Uranium and uranium-based materials are an endless source of unconventional and exotic physical properties: their 5*f* electrons are intermediate between itinerant and localized and experience several interactions (exchange, correlations, spin-orbit, and kinetic) without clean-cut hierarchy. Associated with the large orbital angular moments of these electrons is the possibility also for high-order multipolar electromagnetic asphericities to form and order [1]. The tetragonal heavy fermion superconductor compound URu₂Si₂ is a good example of such materials and has puzzled physicists for more than two decades [2]. Its specific heat presents two anomalies. The first one, at $T_{sc} = 1.2$ K, is ascribed unambiguously to a superconducting transition. The second one, at $T_0 = 17.5$ K, is referred to as a transition to a hidden order (HO), because it is easily recognized in many other macroscopic measurements (nonlinear magnetic susceptibility, thermal expansion, electrical resistivity, etc.) but gives no signal to elastic scattering by neutrons nor by x rays.

The mystery of the HO in URu₂Si₂ remains today unsolved in spite of numerous experimental efforts. No order parameter was experimentally determined for this transition so far. A small staggered antiferromagnetic moment was earlier detected by elastic neutron scattering [3], but this is too tiny to explain the specific heat jump and therefore cannot characterize the HO. One of the present interpretations of this small moment, still debated, is that it is not intrinsic but a residual parasitic contribution coming from a surviving high pressure antiferromagnetic phase with large moments, which is stabilized above 0.6 GPa [4,5]. Recent attempts to search for a possible quadrupolar order by resonant x-ray scattering have failed [6,7]. Several microscopic models, including multipole ordering [8–14], spin-density wave formation [15–17], orbital antiferromagnetism combined with interionic currents [18], and Pomeranchuk instability of the Fermi liquid [19], have been proposed to account for the wide variety of experimental results [2]. Confrontation, however, is lacking with the actual nature of the HO. Its identification would be one

of the most exciting results in the field of heavy fermions, but the task is an experimental challenge. The fact, for instance, that the HO could originate in a freezing of high-rank multipoles cannot be evidenced directly by neutron scattering. Nonetheless, it is reasonable to anticipate that the magnetization distribution induced under an applied magnetic field might depend on the otherwise invisible ground state, in particular if this ground state is not invariant by time inversion. It, thus, became highly desirable to study URu₂Si₂ by polarized neutron scattering on a single crystal under an applied magnetic field in both the paramagnetic phase and the mysterious phase to probe potential relevant changes in the field-induced magnetization distribution when entering the HO.

Precision measurements of the Fourier components $F_M(\mathbf{Q})$, more commonly called (scalar) magnetic structure factors, of a magnetization distribution collinear to an applied magnetic field can be achieved by using polarized neutrons, with the help of the classical polarized beam technique [20]. This consists in measuring the flipping ratio $R(\mathbf{Q}) = I^+(\mathbf{Q})/I^-(\mathbf{Q})$ of the diffracted neutron fluxes at a Bragg scattering vector $\mathbf{Q} = (h, k, l)$ for the polarization of the incoming neutron beam parallel ($I^+(\mathbf{Q})$) and antiparallel ($I^-(\mathbf{Q})$) to the applied field. The method takes advantage of a polarization dependent nuclear-magnetic interference term in the cross section, which allows one to deduce $F_M(\mathbf{Q})$ from $R(\mathbf{Q})$ with great accuracy, at the condition that the nuclear structure is centric and already determined with precision. An unpolarized neutron diffraction experiment is thus a necessary first step. The same single crystal was used for all the experiments reported in this letter. It was prepared by the Czochralski method in a tetra-arc furnace under argon atmosphere and further annealed [7,21], and had a shape of a semidisk ($\sim 5 \times 3 \times 2.5$ mm³).

The unpolarized neutron experiment was carried out on the four-circle diffractometer D9 of the Institut Laue-Langevin, with an incoming neutron wavelength $\lambda = 0.835$ Å. The intensities of 1615 independent reflections,

reducing to a set of 235 symmetry inequivalent observations, were measured at $T = 2$ K and $T = 25$ K up to $Q/4\pi = \sin\theta/\lambda = 1.0 \text{ \AA}^{-1}$. The data were corrected for absorption (with the linear absorption coefficient $\mu = 0.01 \text{ mm}^{-1}$) and the structural parameters were fitted using the Cambridge Crystallography Subroutine Library [22]. The refinements included a Becker-Coppens Lorentzian correction of the extinction [23], that turned out to be extremely strong (a factor 5 for the most extinguished reflections).

Paramagnetic URu_2Si_2 has the ThCr_2Si_2 -type crystal structure (space group $I4/mmm$, $a = 4.112(1) \text{ \AA}$, $c = 9.538(1) \text{ \AA}$ at $T = 25$ K). In this structure, the uranium atoms occupy the $2a$ site (0,0,0), the ruthenium atoms the $4d$ site (0, 1/2, 1/4) and the silicon atoms the $4e$ site (0, 0, z). Much better agreements in the refinements were obtained letting the occupation factor of the ruthenium site free to vary, or equivalently, by mixing silicon and ruthenium on this site as suggested in Ref. [24]. The refinements, taking into account this disorder, led to crystallographic weighted residual factors $R_w(F^2) = 7.5\%$ at the two temperatures. Results are presented in Table I. This disorder affects the ruthenium site only: all the attempts to let the occupation factors of both the uranium or the silicon sites vary led to non significant deviations from unity. This can also be an artefact due to the extremely severe extinction without, however, any consequences on the results of the polarized neutron study.

The flipping ratio measurements have been carried out on the two-axis diffractometer D3, connected to the hot source of the Institut Laue-Langevin. The wavelength of the incoming neutrons was $\lambda = 0.825 \text{ \AA}$ and the polarization $P = 0.95(1)$, set with an Heusler alloy monochromator. Almost perfect polarization reversal was achieved (thanks to Meissner shields). The flipping ratios of 320 independent reflections have been collected under a magnetic field of 9.6 T applied along the magnetization axis \mathbf{c} at 2 K (hidden order) and 25 K (paramagnetic phase), respectively. A set of 50 symmetry-inequivalent magnetic scattering amplitudes $F_M(\mathbf{Q})$ were extracted from the data at each temperature, up to $\sin\theta/\lambda = 0.83 \text{ \AA}^{-1}$ in the

TABLE I. Atomic coordinates, equivalent isotropic Debye-Waller factors, and occupation factors for URu_2Si_2 at $T = 2$ K and $T = 25$ K.

		x	y	z	B_{eq}	Occ.
2 K	U	0	0	0	0.03(1)	
	Ru	0	0.5	0.25	0.06(1)	0.89(1)
	Si ₁	0	0.5	0.25	0.06(1)	0.11(1)
	Si ₂	0	0	0.3730(1)	0.13(1)	
25 K	U	0	0	0	0.04(1)	
	Ru	0	0.5	0.25	0.06(1)	0.88(1)
	Si ₁	0	0.5	0.25	0.06(1)	0.12(1)
	Si ₂	0	0	0.3730(1)	0.15(1)	

reciprocal space. The quantity $F_M(\mathbf{Q} = \mathbf{0})$ cannot be determined with neutrons. As a matter of fact, this describes the macroscopic magnetization and has been measured on a home-build extraction magnetometer. It amounts to $0.178\mu_B/(\text{unit cell})$ at $T = 2$ K and $0.290\mu_B/(\text{unit cell})$ at $T = 25$ K.

To recover the magnetization distribution in real space from the series of $F_M(\mathbf{Q})$ extracted from the measured $R(\mathbf{Q})$, one has to solve an inverse Fourier problem. Several methods can be used [25]. We have first considered a model free analysis of the data and have resorted to the maximum entropy technique (MaxEnt) [26]. This provides the most probable magnetization distribution map compatible with the experimental $F_M(\mathbf{Q})$ and their uncertainties. The method has been shown to give much more reliable results than conventional Fourier syntheses, by considerably reducing both noise and truncation effects. The magnetization distribution in the unit cell has been divided into $64 \times 64 \times 64$ pixels and reconstructed from the experimental $F_M(\mathbf{Q})$, including $F_M(\mathbf{Q} = \mathbf{0})$ that is nothing but the macroscopic magnetization, and using a conventional uniform (flat) prior density. Such a procedure is biased against the creation of any magnetization distribution in the unit cell. Figure 1 shows the reconstructed magnetization distribution in URu_2Si_2 projected along the [001] axis at the two chosen temperatures for the measurements. Note that even though projections of the magnetization distribution along the \mathbf{c} axis are calculated, MaxEnt, on the contrary to a simple inverse Fourier transform, makes use of all the experimental $F_M(h, k, l)$ and not only $F_M(h, k, l = 0)$ [27]. The reconstruction immediately reveals two features that deserve particular attention. The first one concern the ruthenium site: a clear signal, corresponding to an induced magnetization, is visible on this site at the two temperatures. More important is the second feature that concerns the shape of the magnetization distribution around the uranium site: whereas this distribution looks elongated along the [110] and $[1\bar{1}0]$ direction at $T = 2$ K, a change of symmetry is visible when crossing T_0 , with a distribution elongated along [100] and [010] at $T = 25$ K.

In order to get more insight into this shape change of the magnetization distribution at the uranium site when entering the HO, magnetic structure factors $F_M(\mathbf{Q})$ were computed in an ionic model where only uranium is magnetic, from which magnetization distributions were generated by inverse Fourier transform. In the paramagnetic space group $I4/mmm$ (assumed to be still valid even in the hidden order state since we are interested in the ferromagnetic field-induced magnetization),

$$F_M(\mathbf{Q}) = [1 + (-1)^{h+k+l}]T_Q \sin^{-1}(\alpha_Q)E_0(\mathbf{Q}), \quad (1)$$

where T_Q is a temperature factor and α_Q the angle between the Bragg scattering vector $\mathbf{Q} = (h, k, l)$ and the magnetization axis \mathbf{c} . $E_0(\mathbf{Q})$ is the component along \mathbf{c} of the magnetic vector form factor. It is computed from the ionic

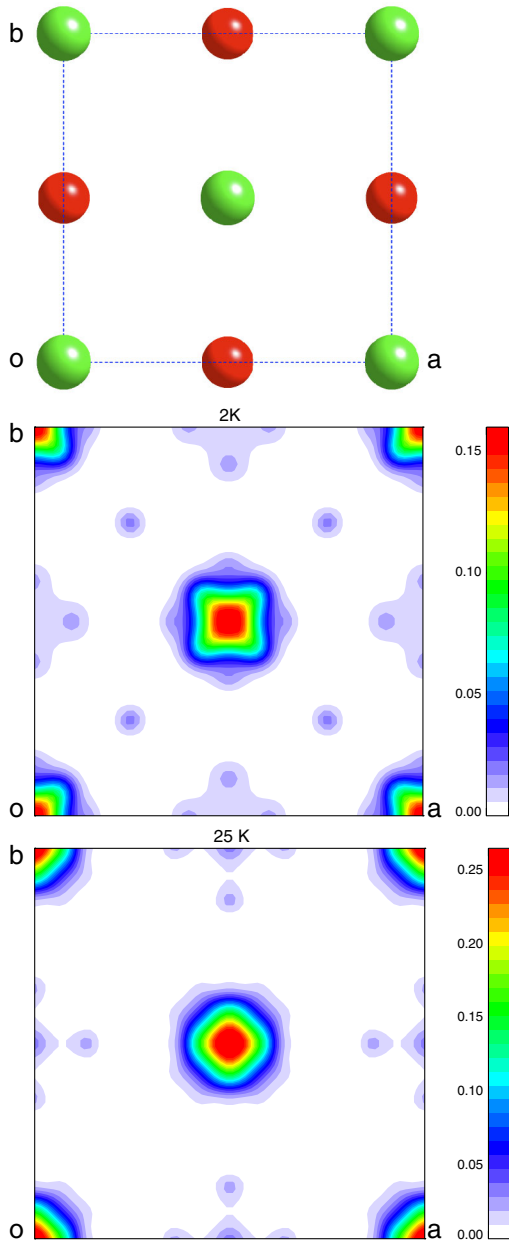


FIG. 1 (color online). Upper: projection of the unit cell of URu_2Si_2 along the crystallographic [001] axis, in the (a, b) plane. Uranium atoms in green, ruthenium atoms in red. Middle: projection of the MaxEnt reconstructed magnetization distribution in URu_2Si_2 along the [001] axis at $T = 2$ K. Lower: same MaxEnt projection at $T = 25$ K.

wave functions of the uranium ions, using the tensor operator formalism [28], and may be written in the form

$$E_0(\mathbf{Q}) = \sum_{K''Q''} Y_{Q''}^{K''}(\hat{Q}) \sum_{K'} \langle j_{K'}(Q) \rangle C_{K''Q''K'}^0, \quad (2)$$

where $Y_{Q''}^{K''}(\hat{Q})$ are spherical harmonics. $\langle j_{K'}(Q) \rangle$ depends only on the radial part of the wave function and is computed for the uranium ions in different valence states from the

relativistic Dirac-Fock Hamiltonian [29]. $C_{K''Q''K'}^0$ depends only on the angular part of the wave function. We, thus, emphasize here that the shape of the magnetization distribution will not be affected, except for some radial dilatation on each uranium position, in the event that the uranium unpaired electrons display some itinerant character but show the same angular momentum states at the Fermi surface as the considered wave functions in the ionic model. On the other hand, the possible hybridization with the other s and d itinerant electrons would alter the $F_M(\mathbf{Q})$ essentially at low modulus of \mathbf{Q} whereas the shape change of the magnetization distribution when entering the HO is to ascribe to the $F_M(\mathbf{Q})$ measured at the largest values of \mathbf{Q} .

A crucial point of the calculations was the choice of the relevant wave functions. First-principle electronic structure computations with dynamical mean-field approximation for correlations [10] suggested that the states with highest weight at the Fermi level correspond to the crystalline electric field singlets

$$\begin{aligned} \Gamma_1^{(1)} &= \frac{1}{\sqrt{2}} \sin\nu(|+4\rangle + |-4\rangle) + \cos\nu|0\rangle \\ \Gamma_2 &= \frac{1}{\sqrt{2}} (|+4\rangle - |-4\rangle) \\ \Gamma_1^{(2)} &= \frac{1}{\sqrt{2}} \cos\nu(|+4\rangle + |-4\rangle) - \sin\nu|0\rangle \end{aligned}$$

built over the states $|M\rangle$ of the ground multiplet $J = 4$ of the $5f^2$ electrons of the U^{4+} ion, within the Russell-Saunders coupling scheme. Generalizing the ionic model reported in Ref. [13], we have considered linear combinations of these singlets in the form:

$$\psi = \cos\alpha\{\cos\varphi\Gamma_1^{(1)} + \sin\varphi\Gamma_1^{(2)}\} + \sin\alpha e^{i\beta}\Gamma_2. \quad (3)$$

The crystalline electric field mixing parameter ν was fixed to 0.998 as in Ref. [13]. Changing this value to another, for instance to a lower one by about 25%, had no qualitative incidence on the computed magnetization distributions. The mixing parameters α and β account for the amount of magnetization distribution and hexadecapolar polarization [13], whereas φ accounts for dotriacontapole polarization. $\Gamma_1^{(1)}$ and $\Gamma_1^{(2)}$ can indeed only be mixed by dotriacontapole operators of the type $J_x J_y J_z (J_x^2 - J_y^2)$. All other multipole operators (quadrupoles, octupoles) have zero matrix element on this state. The macroscopic magnetization computed from ψ is $F_M(\mathbf{Q} = \mathbf{0}) = 2g_J \langle \psi | J_z | \psi \rangle = 2 \times 3.2 \sin(\varphi + \nu) \cos\beta \sin(2\alpha) \mu_B /$ (unit cell). α and β were correlatively varied so as to give the measured macroscopic magnetization for a chosen φ .

The shape of the calculated magnetization distribution for every fixed value of φ turned out to be insensitive to the choice of β : if an hexadecapolar order was stabilized then this would not leave any fingerprint in the field-induced magnetization distribution. As a matter of fact, this is not surprising since hexadecapoles are invariant through time

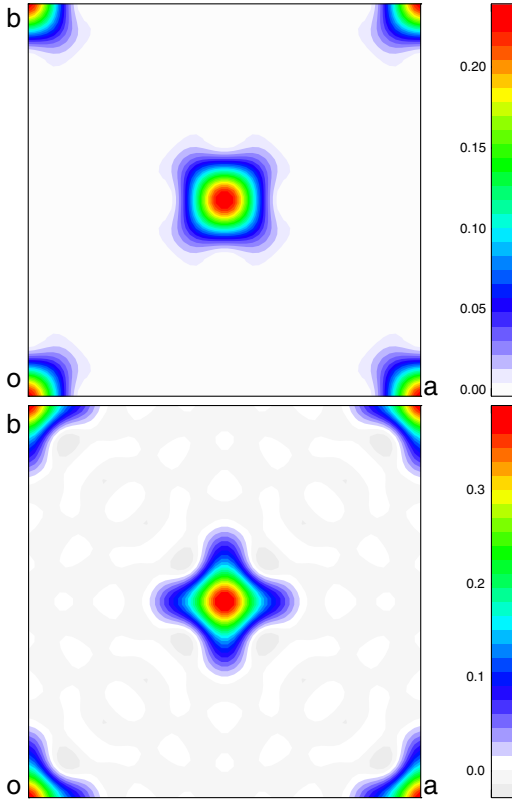


FIG. 2 (color online). Upper: projection of the magnetization distribution calculated from the wave function ψ with $\nu = 0.998$, $\alpha = 0.0165$, $\beta = 0$, $\varphi = 0$ —Lower: projection of the magnetization distribution calculated from the wave function ψ with $\nu = 0.998$, $\alpha = 0.0419$, $\beta = 0$, $\varphi = \pi/2$ [see Eq. (3)].

inversion. Changes in the shape of the calculated magnetization distribution were only found on varying φ . Figure 2 shows the calculated magnetization distribution for $\varphi = 0$ and $\varphi = \pi/2$. When $\varphi = 0$, that is when $\psi = \cos\alpha\Gamma_1^{(1)} + \sin\alpha e^{i\beta}\Gamma_2$, the magnetization distribution is elongated along the $[110]$ and $[1\bar{1}0]$ direction as in the experimentally projected magnetization distribution at 2 K, whereas when $\varphi = \pi/2$, that is when $\psi = \cos\alpha\Gamma_1^{(2)} + \sin\alpha e^{i\beta}\Gamma_2$, the elongation is along the $[100]$ and $[010]$ directions as in the experimentally projected magnetization distribution at 25 K. Since only the wave function ψ is considered, the magnetization distribution in Fig. 2 should be considered as having been computed at zero temperature. This explains why the calculated map for $\varphi = \pi/2$ differs to some extent from the experimental map at 25 K. A few calculations were made with higher energy excited states inferred from the model described in Ref. [13] to incorporate temperature effects, which resulted in the expected smearing in the magnetization distribution. According to the first-principle electronic structure computations reported in Ref. [10], the wave functions with the largest weight in the dynamical mean-field theory density matrix are Γ_2 and $\Gamma_1^{(2)}$, in agreement with our result according

to which the field-induced magnetization distribution at 25 K correspond to the calculated magnetization distribution for $\varphi = \pi/2$. As already emphasized, a change in this mixing parameter φ on decreasing the temperature can be produced only by a dotriacontapole operator, which leads to the conclusion that the mysterious phase in URu_2Si_2 is associated with an order of dotriacontapoles. Recent core spectroscopy experiments suggest that the occupation number of $5f$ electrons would actually be closer to 2.7 [30]. Within the $j - j$ coupling scheme, only 0.7 among them would then occupy the $j = 7/2$ multiplet. The remaining 2, which dominates the band structure near the Fermi level [14], would, however, occupy the $j = 5/2$ multiplet so that the $5f^2$ ionic model we have used is still valid.

To summarize, a shape change in the field-induced magnetization distribution in URu_2Si_2 has been evidenced by accurate polarized neutrons measurements on decreasing the temperature. This effect is unambiguously observed on a very large sample, and on the contrary to experiments that were recently reported to support a nematic phase, is not restrained to very small single crystals and not wiped out by a multidomain structure [31]. Within a simple $5f^2$ ionic model, this shape change is interpreted as a microscopic fingerprint of an order of dotriacontapoles at the origin of the hidden order. Although confrontation to more sophisticated theoretical approaches might be awaited, in particular taking into account the possible itinerant character of the $5f^2$ electrons or considering the alternative scenario of dotriacontapole order with nematic E^- symmetry recently proposed by H. Ikeda *et al.* [14,32], our experimental result already clearly brings to light that the hidden order in URu_2Si_2 is that of dotriacontapoles.

We warmly thank H. Kusunose for fruitful discussion and for providing wave functions and energy levels from the model discussed in Ref. [13], M. Suzuki for communicating results of unpublished band structure calculations, G. Kotliar for useful comments on the experimental results, and H. Ikeda for fruitful discussion on the interpretations and communicating the preprint [14] prior to publication.

-
- [1] P. Santini, S. Carretta, G. Amoretti, R. Caciuffo, N. Magnani, and G. H. Lander, *Rev. Mod. Phys.* **81**, 807 (2009).
 - [2] J. A. Mydosh and P. M. Oppeneer, *Rev. Mod. Phys.* **83**, 1301 (2011).
 - [3] C. Broholm, J. K. Kjems, W. J. L. Buyers, P. Matthews, T. T. M. Palstra, A. A. Menovsky, and J. A. Mydosh, *Phys. Rev. Lett.* **58**, 1467 (1987).
 - [4] E. Hassinger, G. Knebel, K. Izawa, P. Lejay, B. Salce, and J. Flouquet, *Phys. Rev. B* **77**, 115117 (2008).
 - [5] F. Bourdarot, N. Martin, S. Raymond, L.-P. Regnault, D. Aoki, V. Taufour, and J. Flouquet, *Phys. Rev. B* **84**, 184430 (2011).
 - [6] H. Amitsuka, T. Inami, M. Yokoyama, S. Takayama, Y. Ikeda, I. Kawasaki, Y. Homma, H. Hidaka, and T. Yanagisawa, *J. Phys. Conf. Ser.* **200**, 012007 (2010).

- [7] H. C. Walker, R. Caciuffo, D. Aoki, F. Bourdarot, G. H. Lander, and J. Flouquet, *Phys. Rev. B* **83**, 193102 (2011).
- [8] P. Santini and G. Amoretti, *Phys. Rev. Lett.* **73**, 1027 (1994).
- [9] A. Kiss and P. Fazekas, *Phys. Rev. B* **71**, 054415 (2005).
- [10] K. Haule and G. Kotliar, *Nature Phys.* **5**, 796 (2009).
- [11] F. Cricchio, F. Bultmark, O. Granas, and L. Nordstrom, *Phys. Rev. Lett.* **103**, 107202 (2009).
- [12] H. Harima, K. Miyake, and J. Flouquet, *J. Phys. Soc. Jpn.* **79**, 033705 (2010).
- [13] H. Kusunose and H. Harima, *J. Phys. Soc. Jpn.* **80**, 084702 (2011).
- [14] H. Ikeda, M.-T. Suzuki, R. Arita, T. Takimoto, T. Shibauchi, and Y. Matsuda, *Nature Phys.* **8**, 528 (2012).
- [15] H. Ikeda and Y. Ohashi, *Phys. Rev. Lett.* **81**, 3723 (1998).
- [16] V. P. Mineev and M. E. Zhitomirsky, *Phys. Rev. B* **72**, 014432 (2005).
- [17] S. Elgazzar, J. Rusz, M. Amft, P. M. Oppeneer, and J. A. Mydosh, *Nature Mater.* **8**, 337 (2009).
- [18] P. Chandra, P. Coleman, J. A. Mydosh, and V. Tripathi, *Nature (London)* **417**, 831 (2002).
- [19] C. M. Varma and L. Zhu, *Phys. Rev. Lett.* **96**, 036405 (2006).
- [20] R. Nathans, M. T. Pigott, and C. G. Shull, *J. Phys. Chem. Solids* **6**, 38 (1958).
- [21] T. D. Matsuda *et al.*, *J. Phys. Soc. Jpn.* **80**, 114710 (2011).
- [22] P. J. Brown and J. C. Matthewman, in *The Cambridge Crystallography Subroutine Library*, Rutherford Appleton Laboratory, RAL-93-009 (1993).
- [23] P. J. Becker and P. Coppens, *Acta Crystallogr. Sect. A* **30**, 129 (1974).
- [24] P. Lejay, J. Muller, and R. Argoud, *J. Cryst. Growth* **130**, 238 (1993).
- [25] P. J. Brown, *Int. J. Mod. Phys. B* **7**, 3029 (1993).
- [26] R. J. Papoular and B. Gillon, *Europhys. Lett.* **13**, 429 (1990).
- [27] R. J. Papoular, A. Zheludev, E. Ressouche, and J. Schweizer, *Acta Crystallogr. Sect. A* **51**, 295 (1995).
- [28] S. W. Lovesey and D. E. Rimmer, *Rep. Prog. Phys.* **32**, 333 (1969).
- [29] J. P. Desclaux and A. J. Freeman, *J. Magn. Magn. Mater.* **8**, 119 (1978).
- [30] S. Fujimori *et al.*, [arXiv:1110.6689](https://arxiv.org/abs/1110.6689).
- [31] R. Okazaki, T. Shibauchi, H. J. Shi, Y. Haga, T. D. Matsuda, E. Yamamoto, Y. Onuki, and H. Ikeda, *Science* **331**, 439 (2011).
- [32] J. G. Rau and H. Y. Kee, *Phys. Rev. B* **85**, 245112 (2012).